



Constitutive Equation for Gas Sensitivity of Nanocrystalline Tin Oxide Sensor

Satyajit Shukla and Sudipta Seal*

Mechanical Materials Aerospace and Engineering (MMAE), Department and Advanced Materials Processing and Analysis Center (AMPAC) Engineering # 381, University of Central Florida, 4000 Central Florida Blvd., Orlando, Florida, 32816, USA

(Received: 9 April 2004. Revised/Accepted: 17 May 2004)

A new constitutive equation for the gas sensitivity of nanocrystalline tin oxide (SnO_2) thin film sensor is proposed in this investigation. The experimentally observed variation in the gas sensitivity as a function of operating temperature and the amount of reducing gas, as reported in the literature, is shown to be satisfactorily explained by the proposed theoretical model.

Keywords: Author please supply keywords.

Nanocrystalline tin oxide (SnO_2) is a well-known *n*-type semiconductor oxide sensor. When a freshly prepared nanocrystalline SnO_2 thin film is exposed to air, oxygen ions (O_2^- and O^- ions) get adsorbed on the particle surfaces by capturing electrons from the conduction band of SnO_2 . This results in the formation of an electrical double layer on the particle surface, which consists of negatively charged oxygen ions on one side of the surface and positively charged metal ions on the other side. This raises the potential barrier for electron conduction at the grain boundaries, which in turn increases the electrical resistance of the thin film. The captured electrons are, however, returned back to the conduction band, if the reducing gas reacts with the surface adsorbed oxygen ions; thus, reducing the electrical resistance of the thin film.¹

The gas sensitivity of the nanocrystalline SnO_2 sensor, defined as the ratio of its electrical resistance in air (R_{air}) to that in the presence of reducing gas (R_{gas}), depends on number of critical parameters such as nanocrystallite size, film thickness, operating temperature, amount of porosity, amount and nature of dopants, presence of surface catalysts and oxides, and reducing gas concentration. Although

various theoretical models have been proposed^{2–13} to explain the gas sensing characteristics of nanocrystalline SnO_2 sensor, none of the existing models can satisfactorily explain the effect of all variables on the gas sensitivity of nanocrystalline SnO_2 sensor. Thus, the constitutive equation for the gas sensitivity of nanocrystalline SnO_2 thin film sensor is still lacking in the literature. From this point of view, one of the major objectives of the present investigation is to derive the constitutive equation for the gas sensitivity of nanocrystalline SnO_2 thin film sensor.

Recently, we proposed a new theoretical model to explain the nanocrystallite size-dependent gas sensitivity enhancement in nanocrystalline SnO_2 sensor.¹⁴ The experimentally observed gas sensitivity enhancement in nanocrystalline SnO_2 sensor, below 10 nm crystallite size, is satisfactorily explained by this model. In this investigation, we extend our earlier model to show its suitability in explaining the experimentally observed gas sensitivity variation as a function of operating temperature and amount of reducing gas. Thus, a single theoretical equation is derived below, which can satisfactorily explain the effect of three critical variables (nanocrystallite size, operating temperature and amount of reducing gas) on the gas sensitivity of nanocrystalline SnO_2 thin film sensor.

*Corresponding author; E-mail: sseal@pegasus.cc.ucf.edu

1. THEORETICAL MODEL FOR GAS SENSITIVITY VARIATION AS A FUNCTION OF OPERATING TEMPERATURE

In our previous analysis¹⁴ of nanocrystallite size-dependent gas sensitivity enhancement in nanocrystalline SnO₂ sensor, we considered a single crystal of cubic shape of size D , with the space-charge layer thickness, d , perpendicular to the direction of the current flow. Subsequent analysis resulted in the derivation of following expression for the maximum gas sensitivity (S_{\max}) of nanocrystalline SnO₂ sensor,

$$S_{\max} = \frac{2D}{D} \cdot \frac{n_b}{n_{\text{spa}}} \quad (1)$$

where, n_b and n_{spa} are the charge carrier concentrations within the bulk and the space-charge layer in air. The derivation of Eq. 1 is based on number of assumptions,¹⁴ which are valid in the present analysis. Here, we expand Eq. 1 in order to obtain the relationship between the maximum sensitivity and the operating temperature (T).

The space-charge layer thickness, d , is known to be related to the temperature and bulk carrier concentration via a relationship of the form,²

$$d = \sqrt{\frac{\epsilon_r \epsilon_o k T}{q^2 n_b}} \quad (2)$$

where, $\epsilon_r \epsilon_o$ is the permittivity of nanocrystalline SnO₂, k is the Boltzmann's constant and q is the electronic charge. Moreover, the carrier concentration within the space-charge layer in air is related to the bulk carrier concentration via a relationship of the form,¹³

$$n_{\text{spa}} = n_b \cdot \exp\left[\frac{-qV_s}{kT}\right] \quad (3)$$

where, V_s is the potential barrier at the surface. We substitute Eqs. 2 and 3 in Eq. 1.

$$S_{\max} = \frac{1}{D} \cdot \sqrt{\frac{4\epsilon_r \epsilon_o k}{q^2}} \cdot \sqrt{\frac{T}{n_b}} \cdot \exp\left[\frac{qV_s}{kT}\right] \quad (4)$$

The surface potential barrier, V_s , is known to be a function of the occupied surface states, N_s , and donor concentration, N_d , as¹³

$$V_s = \frac{qN_s^2}{2\epsilon_r \epsilon_o N_d} \quad (5)$$

Substituting Eq. 5 in Eq. 4, we get,

$$S_{\max} = \frac{1}{D} \cdot \sqrt{\frac{4\epsilon_r \epsilon_o k}{q^2}} \cdot \sqrt{\frac{T}{n_b}} \cdot \exp\left[\frac{q^2}{2\epsilon_r \epsilon_o k} \cdot \frac{N_s^2}{N_d T}\right] \quad (6)$$

Here we assume that O^- is the dominant occupied surface state; and the oxygen-ion vacancies (with concentration $[V_o]$)

are the donors for the nanocrystalline SnO₂.¹³ Hence, under these conditions, $N_s = [O^-]$ and $N_d = [V_o]$.

Hence,

$$S_{\max} = \frac{1}{D} \cdot \sqrt{\frac{4\epsilon_r \epsilon_o k}{q^2}} \cdot \sqrt{\frac{T}{n_b}} \cdot \exp\left[\frac{q^2}{2\epsilon_r \epsilon_o k} \cdot \frac{[O^-]^2}{[V_o]T}\right] \quad (7)$$

Equation 7 is an expression, which gives the maximum sensitivity of nanocrystalline SnO₂ sensor as a function of a number of parameters such as nanocrystallite size, operating temperature, bulk carrier concentration, density of occupied surface states and concentration of oxygen-ion vacancies.

We further simplify Eq. 7 by substituting,

$$A_1 = \sqrt{\frac{\epsilon_r \epsilon_o k}{q^2}} \quad (8)$$

we get,

$$S_{\max} = \frac{1}{D} \cdot 2A_1 \cdot \sqrt{\frac{T}{n_b}} \cdot \exp\left[\frac{1}{2A_1^2} \cdot \frac{[O^-]^2}{[V_o]T}\right] \quad (9)$$

The dependence of maximum gas sensitivity on the operating temperature for nanocrystalline SnO₂ sensor can be determined via Eq. 9. We observe from Eq. 9 that there are two temperature-dependent terms. The first one is $(T/n_b)^{1/2}$, which is a pre-exponential term and the second one is $[O^-]^2/([V_o]T)$, which is an exponential term. Hence, the second term would primarily determine the operating temperature dependence of the maximum sensitivity of nanocrystalline SnO₂ sensor. Since, the bulk carrier concentration increases with increasing operating temperature and $(T/n_b)^{1/2}$ is a pre-exponential term, it is reasonable to assume, in the present analysis, that the term $(T/n_b)^{1/2}$ is a constant over the operating temperature range considered below.

As shown in Figure 1a, we now consider a single cubic nanocrystal of size $D = 6$ nm and having the space-charge-layer thickness $d = 3$ nm (which is reported at 573 K (300 °C) for nanocrystalline SnO₂ thin film).¹⁵ Under these conditions, the entire particle would be occupied by the space-charge-layer, Figure 1a. Substituting $d = 3$ nm, $\epsilon_r = 13.5$, $\epsilon_o = 8.854 \times 10^{-12}$ C²/Nm², $k = 1.38 \times 10^{-23}$ J/K, $q = 1.6 \times 10^{-19}$ C and $T = 573$ K in Eq. 2, n_b is calculated to be 4×10^{24} m⁻³. (Note: n_b is the bulk carrier concentration when the space-charge-layer is not present, Figure 1b). Moreover, for the above-mentioned conditions, the pre-exponential term in Eq. 9 vanishes and Eq. 9 reduces to,

$$S_{\max} = \exp\left[\frac{1}{2A_1^2} \cdot \frac{[O^-]^2}{[V_o]T}\right] \quad (10)$$

Thus, for the specific case of $D = 6$ nm and $d = 3$ nm, the variation in the maximum sensitivity as a function of operating temperature is given by Eq. 10.

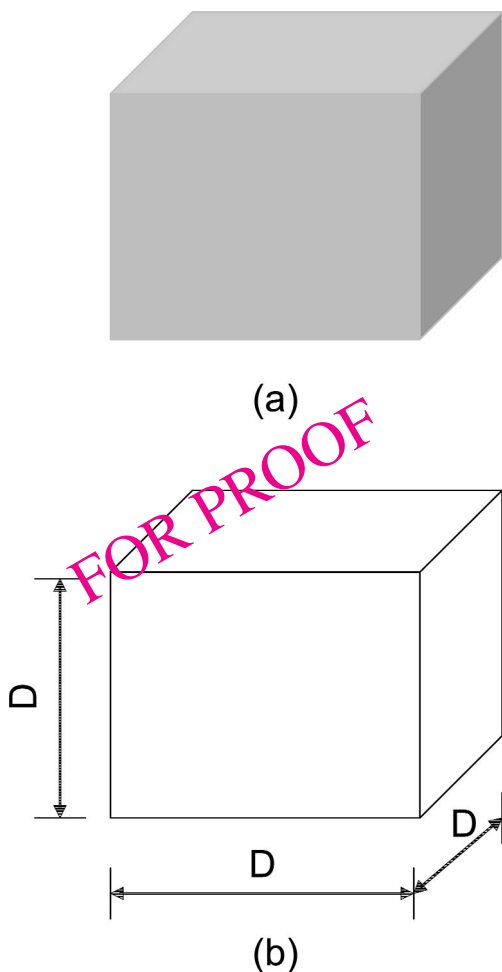


Figure 1. Schematic representation of cubic-shaped single nanocrystal of tin oxide gas sensor, (a) completely occupied by the space-charge layer and (b) without the space-charge layer.

Baik et al.¹⁶ deposited nanocrystalline undoped SnO₂ thin film (dimensions: length = $300 \times 10^{-6} \mu\text{m}$, width = $300 \times 10^{-6} \mu\text{m}$, thickness = $1 \times 10^{-6} \mu\text{m}$), with nanocrystallite size $D = 6 \text{ nm}$, on Al₂O₃ substrate and studied the influence of operating temperature on the hydrogen gas sensitivity. Since, the nanocrystallite size was 6 nm, the observed variation in the hydrogen gas sensitivity as a function of operating temperature can be derived using Eq. 10, by assuming that the observed hydrogen gas sensitivity value at a given temperature is comparable with the maximum one at that temperature.

The data points in Figure 2 represent the experimental variation in the hydrogen gas sensitivity as a function of operating temperature as reported by Baik et al.¹⁶ It appears that hydrogen gas sensitivity increases first, reaches a maximum value, and then decreases with increasing operating temperature within the range of 150–500 °C (423–773 K). The maximum sensitivity value is observed at 350 °C (623 K). The solid line in Figure 2 represents the

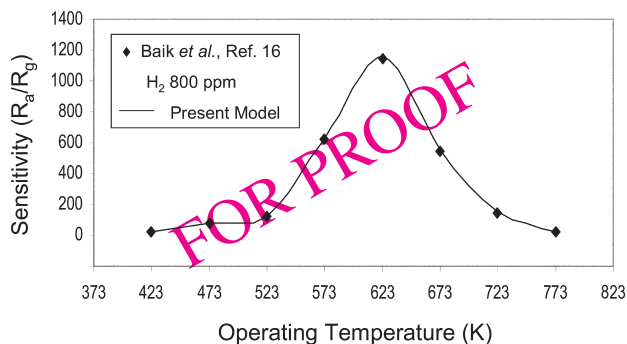


Figure 2. Comparison between the experimental variation¹⁶ of the hydrogen gas sensitivity and the prediction of the present model, Eq. 10, as a function of operating temperature.

theoretical variation in the maximum sensitivity as a function of operating temperature, derived using Eq. 10. Excellent agreement between the theoretical prediction and the experimental values is noted in Figure 2. In order to obtain the perfect fitting between the theoretical prediction and the experimental observations, the assumed variation in the exponential parameter, $[O^-]^2/([V_o]T)$, as a function of operating temperature is shown in Figure 3a. The exponential parameter, $[O^-]^2/([V_o]T)$, is assumed to increase with increasing operating temperature within the range of 150–350 °C (423–773 K). Beyond this range, the exponential parameter, $[O^-]^2/([V_o]T)$, is assumed to decrease with further increase in the operating temperature.

In Figure 3b, we present the assumed variation in the exponential term, $[O^-]^2/[V_o]$, as a function of operating temperature, which is derived using the graph presented in

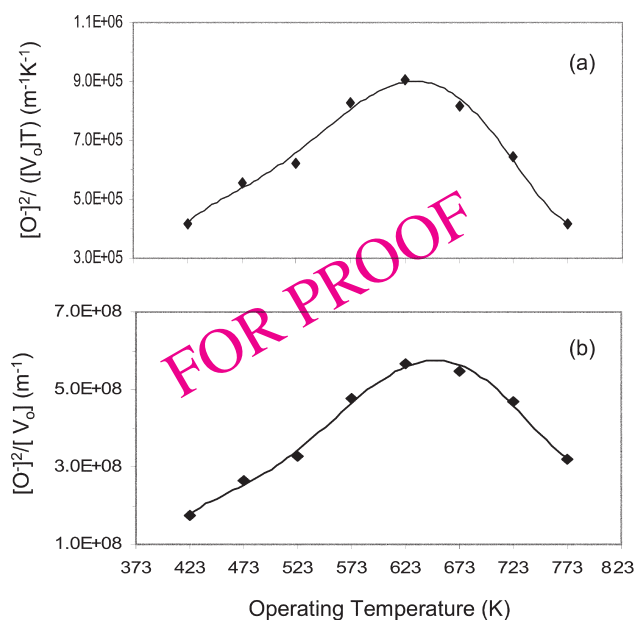


Figure 3. (a) Assumed variation in the exponential parameters, Eq. 10, as a function of operating temperature (b) is derived using (a).

Figure 3a. It appears that the variation in the exponential term, $[O^-]^2/[V_o]$, is similar to that in $[O^-]^2/([V_o]T)$ as a function of operating temperature. Thus, the present model (Eq. 7 or Eq. 10), predicts that the maximum gas sensitivity of nanocrystalline SnO₂ sensor increases initially, Figure 2, due to increase in the value of $[O^-]^2/[V_o]$ with increasing operating temperature, Figure 3b. The decrease in the maximum gas sensitivity with further increase in the operating temperature is a result of decreasing value of $[O^-]^2/[V_o]$ within the high temperature range.

It is to be noted that the validity of the present model is based on the validity (qualitative as well as quantitative) of the assumed variation in $[O^-]^2/[V_o]$ as a function of operating temperature, Figure 3b, which can be justified based on the following two arguments.

First, the lower and the upper limits of total density of surface states, N_t (m⁻²), and the density of donors, N_d (m⁻³), have been tabulated by Ding et al.¹³ Here, the lower and upper limits of N_t^2/N_d are estimated using the reported values as 10^{+6} m⁻¹ and 10^{+14} m⁻¹, respectively. In the present analysis, from Figure 3b, we note that the exponential parameter $[O^-]^2/[V_o]$ is assumed to lie within the range of $1.7 \times 10^{+8}$ to $5.6 \times 10^{+8}$ m⁻¹, which is within the reported range of N_t^2/N_d . The assumed range for the exponential parameter $[O^-]^2/[V_o]$ appears to be closer to the lower limits of N_t^2/N_d . This is understandable due to the fact that N_t refers to the total density of surface states, while $[O^-]$ refers only to the occupied density of surface states. Moreover, the hydrogen sensitivity values reported by Baik et al.¹⁶ may not truly represent the maximum sensitivity values within the given operating temperature range. As a result, the assumed values for the parameter $[O^-]^2/[V_o]$ would lie in between the lower and the upper limits of N_t^2/N_d . This justifies the validity of the present model.

Secondly, the resistance of the nanocrystalline SnO₂ thin film in air (R_{air}) is given by the expression,

$$R_{air} = R_o \cdot \exp\left[\frac{eV_s}{kT}\right] \quad (11)$$

where, R_o is the sensor resistance without the space-charge-layer and V_s is given by Eq. 5. Substituting Eq. 5 in Eq. 11, it can be shown that,

$$R_{air} = R_o \cdot \exp\left[\frac{1}{2A_1^2} \cdot \frac{[O^-]^2}{[V_o]T}\right] \quad (12)$$

Thus, the theoretical variation in the sensor resistance in air as a function of operating temperature can be obtained using Eq. 12. The experimental variation in the sensor resistance in air as a function of the operating temperature, as reported by Baik et al.,¹⁶ is shown in Figure 4a as data points. It is observed that the sensor resistance in air follows the same behavior as exhibited by its hydrogen sensitivity as a function of operating temperature. The theoretical variation in the sensor resistance as a function of

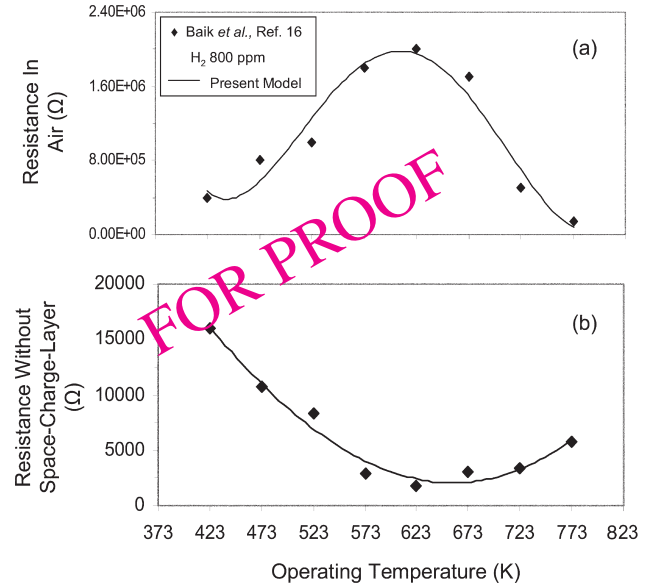


Figure 4. (a) Comparison between the experimental variation¹⁶ of the resistance of nanocrystalline SnO₂ thin film sensor and the prediction of the present model, Eq. 12, as a function of operating temperature. (b) Assumed variation in R_o as a function of operating temperature.

operating temperature, obtained using Eq. 12, is shown as a solid line in Figure 4a. In order to obtain the best fit to the experimental values, appropriate values for the pre-exponential parameter, R_o , are assumed, Figure 4b; while the values for the exponential term $[O^-]^2/[V_o]$ are obtained from Figure 3b.

The resistance of the nanocrystalline SnO₂ sensor without the space-charge-layer is given by the expression,

$$R_o = \frac{1}{n_b q \mu \left(\frac{A}{L}\right)} \quad (13)$$

where, A and L are the cross-sectional area and the length of the nanocrystalline SnO₂ thin film, and μ is the electron mobility (2.0×10^{-4} m²/V·s).¹⁷ Using Eq. 13 and the graph presented in Figure 4b, we determine the assumed values of n_b , which are observed to lie within the narrow range of 2.0×10^{24} to 2.0×10^{25} m⁻³. This is in excellent agreement with the value of 4.0×10^{24} m⁻³, which is assumed at the beginning of the present analysis. This further justifies the validity of the present model.

2. THEORETICAL MODEL FOR GAS SENSITIVITY VARIATION AS A FUNCTION OF AMOUNT OF REDUCING GAS

In the previous investigation,¹⁴ Eq. 1 was derived by assuming that the space-charge-layer is completely eliminated in the presence of reducing gas. As a result, the term

n_{gas} (carrier concentration in the presence of reducing gas) was replaced by n_b to obtain the expression for the maximum sensitivity. Now, we generalize Eq. 1 by re-substituting n_{gas} for n_b and changing the maximum sensitivity (S_{max}) by mere sensitivity (S) term.

$$S = \frac{2d}{D} \cdot \frac{n_{\text{gas}}}{n_{\text{spa}}} \quad (14)$$

Substituting Eqs. 2 and 3 in Eq. 14 and then substituting the expression for V_s (Eq. 5), we get,

$$S = \frac{1}{D} \cdot \sqrt{\frac{4\epsilon\epsilon_o k}{q^2}} \cdot \sqrt{\frac{T}{n_b}} \cdot \frac{n_{\text{gas}}}{n_b} \cdot \exp\left[\frac{q^2}{2\epsilon_r \epsilon_o k} \cdot \frac{[O^-]^2}{[V_o]T}\right] \quad (15)$$

In the literature,^{18, 19} the power law relationship between the sensor resistance and the partial pressure of gases (oxygen and other reducing gases) has been reported. Since, the sensor resistance and the partial pressure of reducing gas are proportional to the charge carrier concentration and the reducing gas concentration, respectively; it is reasonable to assume that the power law relationship also exists between the charge carrier concentration and the reducing gas concentration. Hence, we assume, in the present model, that the latter two parameters are related via the expression,

$$n_{\text{gas}} = n_{\text{spa}} + A_2 \cdot C^n \quad (16)$$

where, C is the amount of reducing gas in ppm and n is the reducing gas concentration exponent. A_2 (m^{-3}) is a parameter, which incorporates two other parameters; the first parameter is proportionality constant and the second one is a parameter that converts the amount of gas in ppm to its concentration. Substituting Eq. 16 in Eq. 15 and assuming that the ratio $n_{\text{spa}}/n_b \approx 0$ as $n_{\text{spa}}/n_b \ll 1$, we get,

$$S = \frac{1}{D} \cdot \sqrt{\frac{4\epsilon\epsilon_o k}{q^2}} \cdot \sqrt{\frac{T}{n_b^{1.5}}} \cdot A_2 C^n \cdot \exp\left[\frac{q^2}{2\epsilon_r \epsilon_o k} \cdot \frac{[O^-]^2}{[V_o]T}\right] \quad (17)$$

This is the final expression showing the relationship between the sensitivity of nanocrystalline SnO_2 sensor and the amount of reducing gas. Equation 17 is also a constitutive equation for the gas sensitivity of nanocrystalline SnO_2 thin film sensor. By substituting appropriate values of ϵ_r , ϵ_o , k , q and $D = 8 \times 10^{-9}$ m, $T = 523$ K (250 °C), $n_b = 4 \times 10^{24}$ m^{-3} , $[O^-]^2/[V_o]T = 623000$ $\text{m}^{-1}\text{K}^{-1}$ (Figure 3a), we obtain,

$$S = (2.0 \times 10^{-12}) \cdot A_2 C^n \quad (18)$$

$$\ln(S) = \ln(2.0 \times 10^{-12} \times A_2) + n \ln(C) \quad (19)$$

Equation 19 predicts that the graph of $\ln(S)$ as a function of $\ln(C)$ must be a straight line, having a slope equal to n .

Now, we consider typical experimental results reported by Hammond and Liu,¹⁷ who studied the effect of the

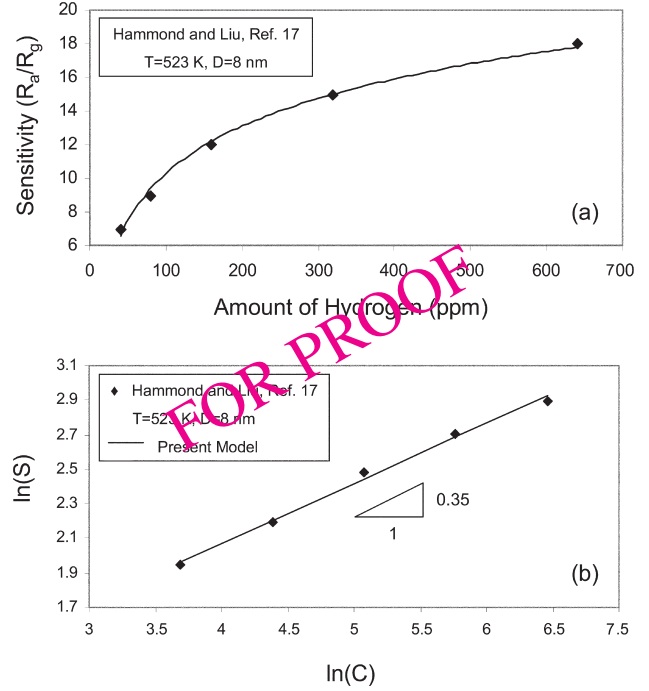


Figure 5. (a) Experimental variation¹⁷ in the hydrogen gas sensitivity of nanocrystalline SnO_2 sensor as a function of the amount of hydrogen gas. (b) Comparison between the experimental variation in the hydrogen gas sensitivity of nanocrystalline SnO_2 sensor and the prediction of the present model, Eq. 19.

amount of hydrogen gas on the hydrogen gas sensitivity of nanocrystalline (8 nm) SnO_2 thin films within the temperature interval of 423–573 K (150–300 °C). Their results reported at 523 K (250 °C) are reproduced in Figure 5a. These experimental results are re-plotted in Figure 5b in a logarithmic scale and are shown by data points. The solid line in Figure 5b is the best-fitted curve, obtained via regression analysis, which can also be described using Eq. 19. The values of n and A_2 in Eq. 19 are, thus, obtained by using the slope and the y-intercept of the best-fitted line and are calculated to be 0.35 and 1.0×10^{12} m^{-3} , respectively.

Further, the experimental variation in the hydrogen gas sensitivity as a function of the amount of hydrogen, as reported for nanocrystalline ($D = 10$ nm) SnO_2 thin film sensor, by Cha et al.,²⁰ is presented in Figure 6a. We substitute $T = 573$ K (300 °C), $D = 10$ nm and $[O^-]^2/[V_o]T = 829750$ $\text{m}^{-1}\text{K}^{-1}$ (Figure 3a), in Eq. 17 (the values of other parameters are the same as above), and obtain following expressions:

$$S = (7.94 \times 10^{-12}) \cdot A_2 C^n \quad (20)$$

$$\ln(S) = \ln(7.94 \times 10^{-12} \times A_2) + n \ln(C) \quad (21)$$

The experimental variation in the hydrogen gas sensitivity as a function of amount of hydrogen, as reported by

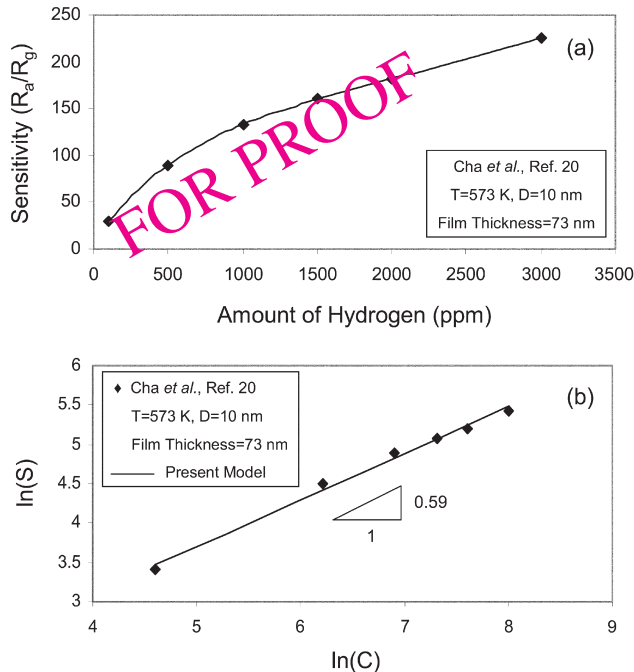


Figure 6. (a) Experimental variation²⁰ in the hydrogen gas sensitivity of nanocrystalline SnO₂ sensor as a function of the amount of hydrogen gas. (b) Comparison between the experimental variation in the hydrogen gas sensitivity of nanocrystalline SnO₂ sensor and the prediction of the present model, Eq. 21.

Cha et al.,²⁰ is re-plotted in Figure 6b in a logarithmic scale and is shown by data points. The solid line in Figure 6b is the best-fitted curve, obtained via regression analysis, which can also be described using Eq. 21. The values of n and A_2 in Eq. 21 are, thus, obtained by using the slope and the y-intercept of the best-fitted line and are calculated to be 0.59 and $0.3 \times 10^{+12}\text{ m}^{-3}$, respectively, which are comparable with those calculated in the previous case. This justifies the validity of the present model.

Thus, in the present investigation, the experimental variation in the gas sensitivity of nanocrystalline SnO₂ sensor as a function of operating temperature and the amount of reducing gas, as reported in the literature, is successfully predicted by developing a constitutive equation (Eq. 17) for the gas sensitivity of nanocrystalline SnO₂ sensor. It is interesting to note that the proposed constitutive equation is also applicable to predict the gas sensing characteristics of other semiconducting oxides such as titania (TiO₂), zinc oxide (ZnO) and tungsten oxide (WO₃), which makes the proposed model more generic in nature.

3. CONCLUSIONS

- (i) A new constitutive equation for the gas sensitivity of nanocrystalline SnO₂ thin film sensor is proposed in this investigation based on a single-crystal model, which satisfactorily explains the as-reported dependence of gas sensitivity of nanocrystalline SnO₂ thin film sensor as a function of three important variables: (a) operating temperature, (b) amount of reducing gas (as demonstrated in this analysis) and (c) nanocrystallite size (as demonstrated in the previous analysis).
- (ii) The proposed constitutive equation may also be useful in explaining the gas sensing characteristics of other semiconducting oxide sensors.

Acknowledgments: The authors thank NASA-Glenn and the National Science Foundation (NSF) for financial support.

References and Notes

1. S. R. Morrison, *The Chemical Physics of Surfaces*; 1st Edition, Plenum Press, New York, NY (1977).
2. N. Barsan and U. Weimar, *J. Electroceramics* 7, 143 (2001).
3. V. Brynzari, G. Korotchenkov, and S. Dmitriev, *Sens. Actuators B* 61, 143 (1999).
4. Y.-S. Choe, *Sens. Actuators B* 77, 200 (2001).
5. Th. Becker, S. Ahlers, Chr. Bosch-v.Braunmuhl, G. Muller, and O. Kiesewetter, *Sens. Actuators B* 77, 55 (2001).
6. G. Sakai, N. Baik, N. Miura, and N. Yamazoe, *Sens. Actuators B* 77, 116 (2001).
7. N. Matsunaga, G. Sakai, K. Shimano, and N. Yamazoe, *Sens. Actuators B* 83, 216 (2002).
8. B. Chwieroth, B. R. Patton, and Y. Wang, *J. Electroceramics* 6, 27 (2001).
9. D. E. Williams and K. F. E. Pratt, *Sens. Actuators B* 70, 214 (2000).
10. M. Ulrich, C.-D. Kohl, and A. Bunde, *Thin Solid Films* 391, 299 (2001).
11. E. Llobet, X. Vilanova, J. Brezmes, D. Lopez, and X. Correig, *Sens. Actuators B* 77, 275 (2001).
12. R. Ionescu, E. Llobet, S. Al-Khalifa, J. W. Gardner, X. Vilanova, J. Brezmes, and X. Correig, *Sens. Actuators B* 95, 203 (2003).
13. J. Ding, T. J. McAvoy, R. E. Cavicchi, and S. Semancik, *Sens. Actuators B* 77, 597 (2001).
14. S. Shukla and S. Seal, *Sens. Letts.* 2, 73 (2004).
15. H. Ogawa, M. Nishikawa, and A. Abe, *J. Appl. Phys.* 53, 4448 (1982).
16. N. S. Baik, G. Sakai, N. Miura, and N. Yamazoe, *Sens. Actuators B* 63, 74 (2000).
17. J. W. Hammond and C.-C. Liu, *Sens. Actuators B* 81, 25 (2001).
18. G. S. V. Coles, G. Williams, and B. Smith, *J. Phys. D: Appl. Phys.* 24, 633 (1991).
19. P. S. More, Y. B. Kholam, S. B. Deshpande, S. R. Sainkar, S. K. Date, R. N. Karekar, and R. C. Aiyer, *Mater. Letts.* 57, 2177 (2003).
20. K. H. Cha, H. C. Park, and K. H. Kim, *Sens. Actuators B* 21, 91 (1994).